



## OPEN Numerical simulation of a forced circulation solar water heating system

Ahmed Remlaoui<sup>1</sup>, Driss Nehari<sup>1</sup>, Benhanifia Kada<sup>2</sup>, Nor Ain Azeany Mohd Nasir<sup>3,4</sup>, Assmaa Abd-Elmonem<sup>5</sup>✉, Neissrien Alhubieshi<sup>5</sup>, Fayza Abdel Aziz ElSeabee<sup>6</sup> & Syed M. Hussain<sup>7</sup>

This study presents a sophisticated numerical simulation model for a forced circulation solar water heating system (FC-SWHs), specifically designed for the unique climatic conditions of Algeria. The model aims to cater to the hot water needs of single-family houses, with a daily consumption of 246 L. Utilizing a dynamic approach based on TRNSYS modeling, the system's performance in Ain Temouchent's climate was scrutinized. The model's validation was conducted against literature results for the collector outlet temperature. Key findings include a maximum monthly average outlet temperature of 38 °C in September and a peak cumulative useful energy gain of 250 W in August. The auxiliary heating system displayed seasonal energy consumption variations, with the highest rate of 500 kJ/hr in May to maintain the water temperature at 60 °C. The energy input at the storage tank's inlet and the consistent high-level energy output at the hot water outlet were analyzed, with the former peaking at 500 W in May. The system ensured an average water tank temperature (hot, middle and bottom) and water temperature after the mixer, suitable for consumption, ranging between 55 °C and 57 °C. For applications requiring cooler water, the mixer's exit temperature was maintained at 47 °C. The study's key findings reveal that the TRNSYS model predicts equal inlet and outlet flow rates for the tank, a condition that is particularly significant when the system operates with high-temperature water, starting at 55 °C. The flow rate at this temperature is lower, at 7 kg/hr, while the water mass flow rate exiting the mixer is higher, at 10.5 kg/hr. In terms of thermal performance, the system's solar fraction (SF) and thermal efficiency were evaluated. The results indicate that the lowest average SF of 54% occurs in July, while the highest average SF of over 84% is observed in September. Throughout the other months, the SF consistently stays above 60%. The thermal efficiency of the system varies, ranging from 49 to 73% in January, 43–62% in April, 48–66% in July, and 53–69% in October. The novelty of this research lies in its climate-specific design, which addresses Algeria's solar heating needs and challenges. Major contributions include a thorough analysis of energy efficiency metrics, seasonal auxiliary heating demands, and optimal system operation for residential applications, supporting Algeria's goal of sustainable energy independence.

**Keywords** Forced circulation solar water heating system, Thermal efficiency, TRNSYS modelling, Numerical results, Solar fraction, Auxiliary heating system, Algeria climate

### Symbols

$SF_d$ and $SF$	Daily and total solar energy factors
$I_T$	Incident total solar radiation, kJ/hr m <sup>2</sup>
A	Total area of the solar collector array or membrane area, m <sup>2</sup>

<sup>1</sup>Applied Hydrology and Environment Laboratory, University of Ain Témouchent -BELHADJ Bouchaib, 46000 Ain-Témouchent, Algeria. <sup>2</sup>Faculty of Science and Technology Laboratory of Energy in Arid Region (ENERGARID), University of Tahri Mohamed Bechar, 08000 Bechar, Algeria. <sup>3</sup>Department of Mathematics Centre for Defence Foundation Studies, Universiti Pertahanan Nasional Malaysia, Kem Sungai Besi, 57000 Kuala Lumpur, Malaysia. <sup>4</sup>Institute for Mathematical Research Laboratory of Computational Sciences and Mathematical Physics, Universiti Putra Malaysia, 43400 UPM Serdang, Selangor, Malaysia. <sup>5</sup>Department of Mathematics College of Science, King Khalid University, Abha, Saudi Arabia. <sup>6</sup>Department of Mathematics College of Science, Qassim University, 51452 Buraydah, Saudi Arabia. <sup>7</sup>Department of Mathematics Faculty of Science, Islamic University of Madinah, 42351 Madinah, Saudi Arabia. ✉email: aahaasn@hotmail.com

$a_0$	Intercept efficiency
$a_1$	Efficiency slope, kJ/hr m <sup>2</sup> K
$a_2$	Efficiency curvature, kJ/hr m <sup>2</sup> K <sup>2</sup>
Qu	Useful thermal energy, W
T	Temperature, K
$T_{in,col}$	Inlet collector temperature, K
$T_{out,col}$	Outlet collector temperature, K
$T_a$	Ambient (air) temperature, K
$C_p$	Specific heat of fluid, kJ/kg K
$\dot{m}$	Mass flow rate, kg/s
$Q_{aux}$	Auxiliary energy, W
$Q_{u,annual}$	Annual useful energy, W
$Q_{load}$	The energy requirement of the load, W
$Q_{loss}$	The energy losses from the storage tank and the piping system, W
$Q_{sup,HX}$	The energy supplied by the heat exchanger, W
$Q_{delivered}$	The energy extracted via the tank's outlet, W
$M_i$	Mass of water in node i, kg.
$Q_{env}$	The energy exchanged via convection with surrounding air, W
$Q_{cond}$	The energy exchanged via conduction between two layers, W
$Q_{inject}$	The energy associated with the inoculation of cold or hot water into the system, W
$Q_{flue}$	The energy convective exchanged with a potential chimney, W
$T_{wout,ave}$	The average temperature of the hot water delivered to the load, K
V	wind velocity, m/s
<b>Greek</b>	
$\eta_{th}$	Efficiency, %
$\eta_{sys}$	system effectiveness, %
$\eta_{coll}$ and $\eta_{coll-d}$	Overall and daily simulation efficiencies of the collector, %
<b>Abbreviations</b>	
SWHs	Solar water heating systems
FC-SWHs	Forced circulation solar water heating system
TRNSYS	Transient System Simulation program
ICS	Integral collector-storage
FPCs	Flat plate collectors
ETCs	Evacuated tube collectors
HTF	Heat transfer fluid
TMY	Typical Meteorological Year
HX	Heat Exchanger

Algeria's solar possibility is a benefit for the residential area, suggesting an ecological solution to resources requirements through solar water heating systems (SWHs). These systems is the bargaining chip of country's high solar irradiance, which can extensively cut dependency on common energy sources, with some provinces attaining thermal energy endowment of up to 85.6%<sup>1</sup>. The efficient utilization of SWHs associates with global climate change modification attempts, possibly saving substantial CO<sub>2</sub> releases yearly<sup>2,3</sup>. As a proof to Algeria's pledge to renewable energy and environmental stewardship, SWHs are progressively credited for their productivity in meeting domestic hot water requests, tributary to the drop of fossil fuel support and releases<sup>3</sup>. Techno-economic examines uphold the feasibility of SWHs, placing them as a convincing selection for Algeria's quest of sustainable energy solutions<sup>4</sup>. The raising requirement for effective SWHs is driven by the nation's rising energy needs, urged by economic development, and growing living standards, specifically helping single-family households<sup>2</sup>. Notwithstanding these benefits, challenges continue, comprising the optimization of solar collector positions and adjustment to Algeria's varied climate and energy requires<sup>1,5</sup>. Economic reasons, such as Algeria's minimal fuel rates, impose government funding to help the shift towards renewable energy<sup>1</sup>. Likewise, the absence of incorporation of international standards for energy and environmental implementation in design and construction is an obstacle to the prevalent approval of SWHs<sup>6</sup>. Conquering these barriers is critical for utilizing the full ability of SWHs in Algeria, thereby advocating the nation's sustainable energy goals.

SWHs are a renewable energy machinery that confines solar energy to heat water for domestic, commercial, or industrial usage. SWHs are classified into two main classes: active and passive. Active systems utilize pumps and controls to mix water or a heat transportation fluid over the system and are sectioned into straight circulation systems, which are appropriate for non-icy weathers, and subsidiary circulation systems, which are planned for icy circumstances. Passive systems, which count on natural convection, consist of integral collector-storage (ICS) systems for mild-icy temperatures and thermosyphon systems where water emerges through the system as it is warmed. Between active systems, forced circulation systems exceptionally superior for their effectiveness and control. These systems dynamically pump the heat transportation fluid over the solar collectors and into a heat exchanger or immediately into the storage reservoir. This method is remarkably useful in miscellaneous climates, involving those with icy temperatures, as it blocks the fluid from icy and grants for specific temperature control<sup>7</sup>. The optimization of such systems can substantially boost their performing, making them a vigorous solution for environmental hot water source<sup>8</sup>. The simulation of enforced motion solar water heating systems (FC-SWHs) grants for enormous manipulation over the system's process. Latest findings have persistent on improving FC-SWHs for energy achievement and economic profits, using methods alike genetic algorithms to boost life cycle cost values<sup>7</sup>. Differences with extra systems, such as thermosyphon solar water heaters, have demonstrated the

FC-SWHs can attain superior thermal productivities ( $\eta_{th}$ ) and solar fractions (SF), implying an additional dependable attainment<sup>8</sup>. These systems are at the limelight of solar heating equipment, suggesting a competent and environmental results for gathering hot water requests in countless locations. Abundant simulation and experimental findings have been performed on FC-SWHs, exhibiting their effectiveness and adaptableness throughout several weathers<sup>9</sup>. This research insists the function of FC-SWHs in enhancing environmental energy results.

The investigation which is caused by Allouhi et al.<sup>9</sup> displayed a solar water heating system with hot pipe-flat plate collectors (FPC) that executed effectively beneath difficult climate requirements. The system's thermal efficacy rouse to 33%, and exergetic competence was around 4%, with everyday SF throughout 58% thru the freezing month in Fez, Morocco. Enhancing the number of heat pipes to 15 within the collector extensively superior operation, with average daily  $\eta_{th}$  in January around 48% and exergetic competences between 4% and 8%. Wangchuk et al.<sup>10</sup> have operated a thorough simulation of active FC-SWHs. The system covered five FPC and a 500-litre water storage capacity tank provided with a heat exchanger. Their discoveries exposed that raising the hot tank's temperature from 60 °C to 80 °C caused in a two-hour expansion of the stagnation time. This modification granted the system to yield 25.425 kWh of thermal energy, a substantial improves from 18.45 kWh at the lower temperature. Furthermore, this alter augmented the system's total productivity from 27.13 to 37.88%.

Numerous studies have explored simulated solar water heating systems (SWHs) with different configurations to enhance efficiency, cost-effectiveness, and sustainability. These simulations involve varying collector types—such as flat-plate, evacuated tube, and photovoltaic (PV) systems—and integrating Latent Heat Thermal Energy Storage (LHTES) units. Researchers have investigated factors like seasonal weather impacts, efficiency, cost, environmental footprint, and overall sustainability to identify optimal SWH designs. For instance, Ibrahim et al.<sup>11</sup> examined how South Africa's distinct four-season climate affects SWH performance. Using Matlab Simulink, they simulated the system with historical weather data from Pretoria, showing that seasonal solar intensity shifts lead to temperature variations in the absorber and storage tank. Their study revealed that, although the highest storage temperatures occur in spring and the lowest in winter, the SWH system still reliably meets hot water needs throughout the year. In another study, Laasri et al.<sup>12</sup> enhanced SWH efficiency by incorporating a Topology-Optimized Latent Heat Thermal Energy Storage (TO-LHTES) unit with fins, tested with EnergyPlus and CFD. They found that using Phase Change Materials (PCMs) like RT50, under specific temperature and flow conditions, improved energy savings by up to 63.2%, making it a promising approach for efficient heat storage and distribution. Hachchadi et al.<sup>13</sup> compared flat-plate, evacuated tube, and PV-based SWHs based on efficiency, cost, and environmental impact. Their findings highlighted that while PV water heaters had lower thermal efficiency, they were the most cost-effective, with a leveled cost of 0.14–0.23 CAD/kWh, though PV systems had a higher lifetime CO<sub>2</sub> output than solar thermal options. This study emphasizes the need to balance cost savings with environmental considerations when selecting SWH systems. Finally, Suwaed et al.<sup>14</sup> studied SWH feasibility for households in Kirkuk, Iraq, to promote sustainability and reduce non-renewable energy dependence. Using T\*SOL software, they analyzed systems with different collector types and storage tanks. Results indicated that evacuated tube collectors in an open-loop setup covered 86% of energy needs and required a smaller tank, cutting CO<sub>2</sub> emissions by up to 1316 kg/year, thus proving SWH systems as viable, sustainable alternatives to electric water heating.

A FC-SWHs supplied with FPCs was thoroughly examined. The examination used the Polysun simulation tool to model the system and determine key performing parameters such as sensible heat, thermal yield, energy supply,  $\eta_{th}$ , system effectiveness ( $\eta_{sys}$ ), and SF. This thorough modelling method was authenticated against empirical measurements, guaranteeing the simulation's precision. The outcomes were favourable, displaying a strong correlation between the simulated data and actual performance accomplished by Maraj<sup>15</sup>. Qing et al.<sup>16</sup> commenced a massive assessment of two variants of FC-SWHs: one incorporating a heat exchanger and the other devoid of it. Through numerical simulations, they explored the dynamic changes in water heat intimate the stowage tanks and evaluated how the size of the heat exchanger influenced the system's thermal efficiency. They also scrutinized different pump control strategies to ascertain the most effective one. In addition to the simulations, the researchers constructed an actual solar water heating system with a temperature exchanger to conduct empirical tests, thereby corroborating their simulation model.

A multitude of computational frameworks have been established to systematically evaluate the long-term efficacy of FC-SWHs in single-family residences, as well as to examine the impact of design elements. This broad and varied body of work mirrors the escalating interest in eco-friendly energy alternatives. TRNSYS 17 (a TRaNsient Systems Model Sequencer)<sup>17</sup>, is a comprehensive tool for the transient model of solar schemes, whether thermal or photovoltaic, as well as multi-zone buildings, renewable energy systems, fuel cells, and low-energy solar equipment. This software has gained widespread adoption for the investigation and refinement of solar systems. Research utilizing TRNSYS typically zeroes in on the system's design, enhancement, and performance assessment across different weather conditions. In the research conducted by Mabrouki et al.<sup>18</sup>, the focus was on assessing the energy requirements of a solar combi-system for a type F3 dwelling in Meknes, Morocco. The team employed the Regulatory Technical Document to ascertain the heating needs and ensure adherence to thermal regulations. They estimated the household hot water query using an analytical method, which was consequently justified by thermal simulations using TRNSYS 16. The findings emphasized the combi-system's volume to collect a significant portion of the hot water heating requirements over an increased time, thus providing to the decrease of greenhouse gas releases. Furthermore, computed solutions from the findings denoted that the system could substantially compensated traditional energy utilization, with the possibility to prepare a better, extra environmental solution for household hot water creation<sup>18</sup>.

A fundamental research in the area overseen a dynamic simulation and energy assessment of FC-SWHs in two different climatic cities of Iraq<sup>19</sup>. The study exploited the TRNSYS to discover the stratification impact inside

the storage tank on the  $\eta_{th}$  and the effect of household hot water management on the  $\eta_{sys}$ . The outcomes from the model specified that, the system in Basrah attained the maximum SF values, assigned to the region's plentiful solar energy, with a standard SF of 66% during winter. The  $\eta_{sys}$  in transforming solar energy to heat water was witnessed to be amongst 67–81% in summer and 39–62% in winter for Baghdad, and between 69 and 82% in summer and 49–66% in winter for Basrah. In the freezing months, the extreme supporting energy involved was 2980 MJ/month in Baghdad and around 2607 MJ/month in Basrah<sup>19</sup>.

In the investigation guided by Abdunnabi et al.<sup>20</sup>, a detailed assessment of the TRNSYS simulation software's precision was conducted out, precisely aiming on its ability to simulate various setups of FC-SWHs. These systems were distinguished by 200 L storage tanks and evacuated tube collectors (ETC). The research carefully explored the elements that could trigger changes between the simulated calculations and the real experimental results. Preliminary experiments implied some irregularities, which were generally recognized to the locating of the temperature sensors that are important for supervising the pump's movement. The breakthroughs endorsed that the TRNSYS program offered satisfactory estimations when contrasted to the experimental data. The difference in the daily energy produce from the system was retrieved to be fewer than 20.2%, and the difference in calculating the hot water outlet temperature was beneath 16%. Particularly, the evacuated tube collector model inside TRNSYS gotten estimate outcome with a precision beyond 13.5%<sup>20</sup>. Yan et al.<sup>21</sup> persistent on improving SWHs through TRNSYS simulations, reviewing the induce of several collector areas and water tank volumes on the system's effectiveness and solar energy assurance ratio. These findings cooperatively emphasize the ability of necessary movement solar water heating assemblies to specify a consistent and competent source of thermal energy for single-family households, specifically in areas with rich sunlight. They also highlight the significance of simulation tools like TRNSYS in planning and improving these systems for extreme effectiveness and sustainability. The literature review suggests a convincing trajectory concerning more innovative and effective solar water heating solutions that can substantially provide to lowering global energy utilization and greenhouse gas radiations. In the correlative analyze by Sakellariou et al.<sup>8</sup>, the energy efficacy of a forced-circulation solar water heating system was assessed preposition a similar thermosyphon system. Both systems were installed in parallel and faced the same level of household hot water requirement. The investigate showed that under unique weather environment, the systems executed comparably in terms of SF and  $\eta_{th}$ . Conversely, during continual operational period of four days, the forced-circulation system showed greater accomplishment, reaching an SF of 0.62 and  $\eta_{th}$  of 68.2%, as countered to the thermosyphon system's SF of 0.48 and  $\eta_{th}$  of 53.3%.

The primary goal of this research is to progress a sophisticated numerical model exemplary aimed at an obligatory movement solar water heating structure, meticulously tailored to the unique climatic conditions prevalent in Algeria. This model seeks to accurately forecast the scheme's performance while accounting for the region's unique solar radiation patterns and atmospheric variables. By simulating various scenarios and configurations, the model will serve as a vital tool in optimizing the design and operation of these systems for single-family houses. The anticipated benefits are multifold: enhanced energy efficiency, maximized utilization of solar energy, and a significant reduction in both energy costs and carbon footprint. Such advancements could revolutionize the way solar energy is harnessed in residential settings, propelling Algeria towards a more sustainable and energy-independent future.

This research is constructed to systematically discover the difficulties of a forced circulation solar water heating system appropriate for Algerian single-family households. It reveals as follows: In the [materials and methods](#) section, household hot water systems are proposed, describing their thermal working and energy analysis to set the stage for following modeling. Inducing to modeling the household hot water system, TRNSYS 17 simulations are described, establishing the backbone of the study, and describing the simulation process along with the parameters contemplated for precisely modeling the system. The outcomes and discussion section concealments numerous parts, comprising model validation against empirical data, valuation of meteorological data disturbing system effectiveness, discussion on efficiency metrics such as monthly average collector outlet temperatures, cumulative useful energy gain, and efficacy differences throughout the year. Furthermore, it examines storage tank dynamics and system flow rates. The article aims to illuminate the potential of solar water heating systems in Algeria, providing a blueprint for optimizing system performance and energy efficiency.

## Materials and methods

### Domestic hot water system

The solar water heating system is a way, to sunlight and converts it into heat energy for warming water. It usually consists of these parts; The Flat Plate Collector (FPC) acts as the core of the setup absorbing the sun's energy and passing it on to the fluid for carrying heat. Additionally, the Storage Tank holds onto the fluid from the collector ensuring that the water remains hot until it is required. To facilitate movement, between the collector and storage tank a Circulating Pump is utilized. On a rainy day or a few no-sunlight hours, an Electric Auxiliary Heater serves as a backup to maintain constantly hot water for use. The system also includes a Differential Temperature Controller monitor of the collector's temperature and the storage tank's temperature. When the collector's temperature is higher than that of the storage tank, the circulating pump is set to function. A Thermostatic Mixing Valve safety device that blends the hot water from the storage tank and cold water to ensure no scalds. The SWH system works by running a heat-transfer fluid, typically water or antifreeze solution, through the flat plate collector to get heated by the sun. Once heated, the fluid flows to the storage tank to release the heat to the water through a heat exchanger. The function of the differential temperature controller is to stop the fluid circulation unless there is enough heat to be transferred. The thermostatic mixing valve is crucial in maintaining the user's safety by stopping the flow of overly hot water to the tap, which can cause scalding. A schematic diagram of the complete SWH system is illustrated in Fig. 1, providing a visual representation of the interconnections and flow paths within the system. This diagram is crucial for understanding the operation and maintenance of the SWH system.

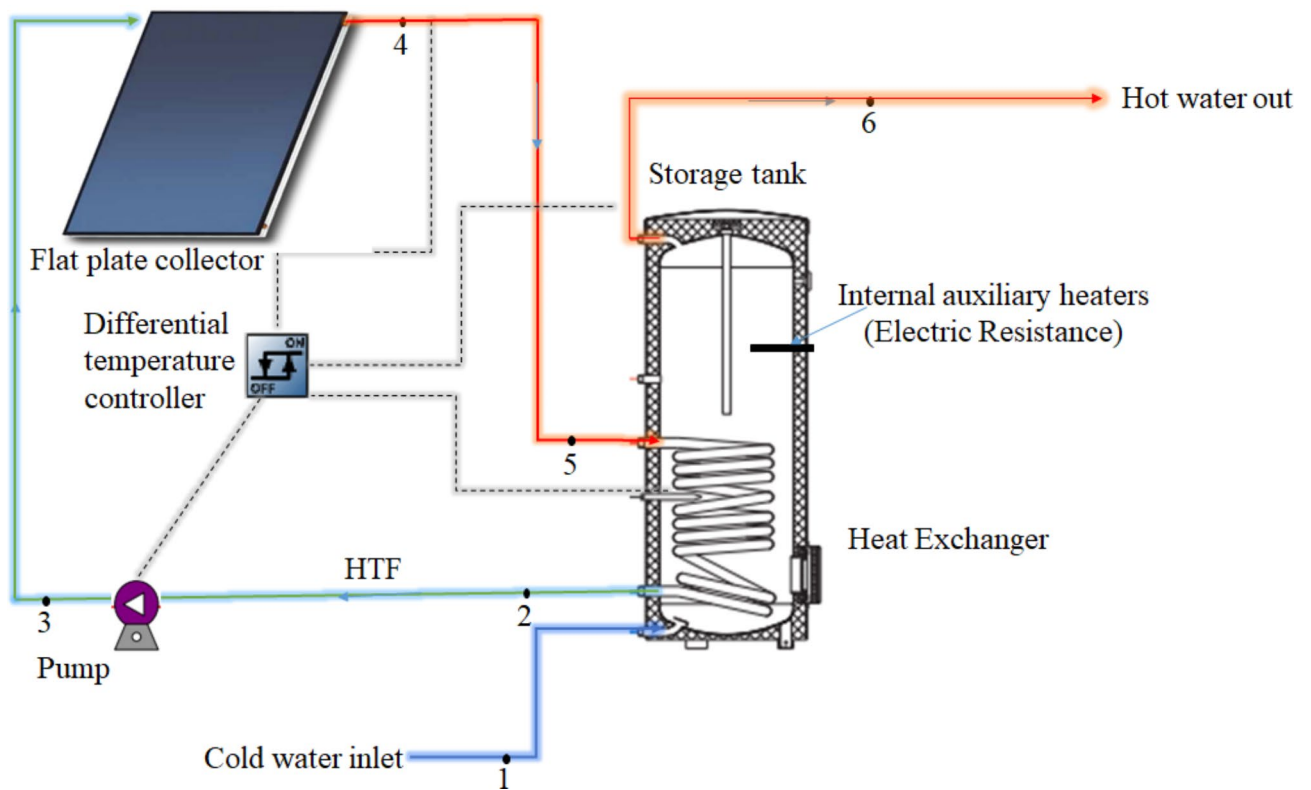


**Fig. 1.** Diagram of the forced circulation solar water heating system model.

### Hot water load outline

A complex topic, the hourly distribution of hot water use during the day is influenced by a variety of factors, including daily, seasonal, and familial ones. The research currently in publication has examined a variety of cyclic load patterns, including constant, early morning, early afternoon, late morning, and late afternoon. A family's typical hot water usage differs significantly depending on a variety of factors, including the number of people residing in the apartment, their schedules, and some cultural variances. The hot water use of 246 L per day in this paper is dispersed throughout the day based on the Rand profile, as seen in Fig. 2<sup>22</sup>.

### Thermal performance and energy analysis

The Flat Plate Collector (FPC) solar water heating system is an active commercial one that comprises an FPC collector, a pump, and storage tank as shown in Fig. 1. The whole installation has the necessary control strategy.

The fundamental equation determining the efficiency of a solar thermal collector is derived from the Hottel-Whillier equation<sup>23</sup>.

$$\eta_{coll} = \frac{Q_u}{A I_T} = a_0 - a_1 \frac{(T_c - T_a)}{I_T} - a_2 \frac{(T_c - T_a)^2}{I_T} \quad (1)$$

Where:  $I_T$  represents the incident total solar radiation measured in  $\text{kJ/hr/m}^2$ , which is the total solar energy received per hour per square meter,  $Q_u$  denotes the beneficial current dynamism which is relocated from the solar energy to the Heat Transfer Fluid (HTF) as it passes through the Flat Plate Collector (FPC), expressed in W. The thermal efficiency of the collector is characterized by three coefficients:  $a_0$ ,  $a_1$ , and  $a_2$  are known as the intercept efficiency (indicating the efficiency of the collector at the reference condition), the efficiency slope (representing the first-order coefficient in the collector efficiency equation)  $\text{kJ/hr/m}^2/\text{K}$  and the efficiency curvature (the second-order coefficient in the collector efficiency equation), with  $\text{kJ/hr/m}^2/\text{K}^2$  respectively;  $T_{in,col}$  is the fluid heat at the inlet to the collector (K) and  $T_a$  is the ambient (air) temperature (K). Equation 2 is utilized to determine  $Q_u$ , this energy is a measure of the system's ability to convert incident solar radiation into usable heat,  $T_{out,col}$  is the fluid heat at the outlet to the collector (K)<sup>23</sup>.

$$Q_u = \dot{m}_{HTF} C_{p,HTF} (T_{out,col} - T_{in,col}) \quad (2)$$

The annual useful energy is calculated based on various factors, including the total amount of solar radiation received, the efficiency of the solar collector, and the performance of the system throughout the year. This energy signifies the sum measure of heat energy that is efficiently consumed throughout a year, is attained from<sup>23</sup>.

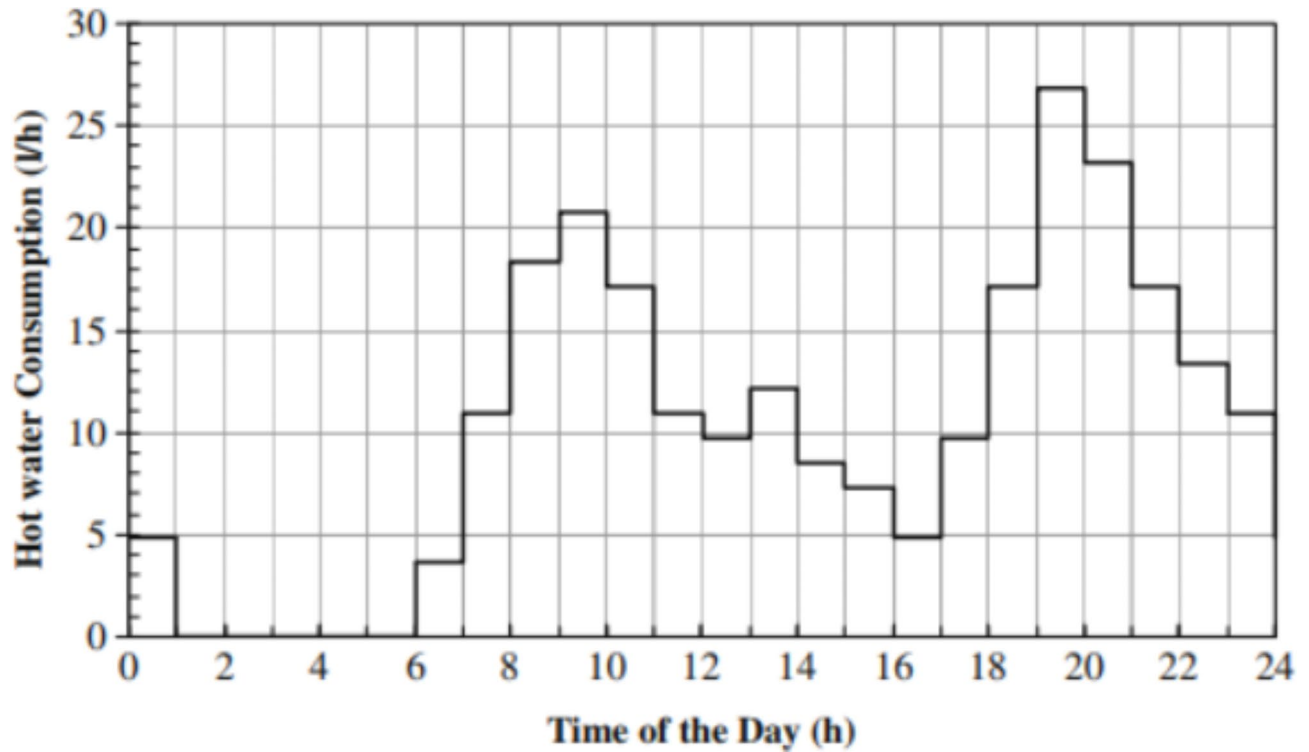


Fig. 2. Profile of daily hot water usage (246 L/Day) as researched by Hobbi and Siddiqui<sup>22</sup>.

$$Q_{u,\text{annual}} = \sum_{d=1}^{365} \sum_{h=1}^{24} Q_u \quad (3)$$

The auxiliary energy ( $Q_{aux}$ ) is the supplementary energy required when the solar collector unable to contribute sufficient heat to increase the water to the required temperature. This circumstance happens thru periods of insufficient solar radiation. The calculation of ( $Q_{aux}$ ) considers:  $Q_{load}$ : The energy requirement of the load, which is the quantity of energy necessitated to achieve the heating demands.  $Q_{loss}$ : The energy losses from the storage tank and the piping system. By contemplating these factors,  $Q_{aux}$  guarantees that the water gets the necessary temperature even when solar energy is inadequate from<sup>23</sup>.

$$Q_{aux} = Q_{load} - (Q_{u,\text{annual}} - Q_{loss}) \quad (4)$$

The solar fraction (SF) is a critical metric for measuring the execution of a thermal system, exceptionally in terms of its involvement to water heating. It signifies the ratio of the total dynamism demand for domestic hot water that is linked via solar energy. The SF considers the total dynamism requirement via the load (which is the energy extracted via the tank's outlet  $Q_{delivered}$ ), incorporating both the energy diminishing returns inside the system and the energy preserved remaining to the solar collectors' effectiveness. When the output from the solar collectors is inadequate to satisfy the entire energy demand of the load, auxiliary energy ( $Q_{aux}$ ) is utilized. The formula for calculating the solar fraction, as provided by in<sup>24</sup>, is as follows:

$$SF = \frac{Q_{aux} + Q_{delivered}}{Q_{delivered}} = 1 - \frac{Q_{aux}}{Q_{delivered}} \quad (5)$$

The storage tank is equipped with an interior temperature exchanger designed to engross the valuable dynamism from the Heat Transfer Fluid (HTF). Additionally, it contains internal heaters that are activated to supplement energy whenever necessary. The energy balance of the system, considering these components, is encapsulated in the following equation<sup>25</sup>:

$$M_i C_p \frac{dT}{dt} = Q_{env} + Q_{cond} + Q_{sup,HX} + Q_{aux} + Q_{inject} + Q_{flue} \quad (6)$$

Where  $C_p$  is the detailed temperature of the water controlled in the storing tank, expressed in kJ/kg/K,  $M_i$  indicates the mass of water in bulge I (kg),  $Q_{env}$  is the energy flow exchanged via convection between the storage tank and the surrounding air, measured in (W),  $Q_{cond}$  represents the dynamism movement exchanged by conduction between two layers (W),  $Q_{inject}$  is the energy flow associated with the inoculation of cold or hot water into the system (W), and  $Q_{flue}$  is the convective energy flow exchanged with a potential chimney (W).

The following formula<sup>26</sup> determines how much heat the solar water heating system transfers from the storage tank to the load:

$$Q_{\text{delivered}} = \dot{m}_w C_{p,w} T_{wout,ave} \tag{7}$$

Referring to Eq. (7), the term  $\dot{m}_w$  represents the mass flow rate of water (kg/hr),  $C_{p,w}$  stands for the specific heat capacity of water (kJ/kg·K) and  $T_{wout,ave}$  indicates the average temperature of the hot water that is delivered to the load (K).

### TRNSYS model of forced circulation solar water heating system

Figure 3 is a schematic diagram that shows how a forced circulation solar water heating system (FC-SWHs) works. This model illustrates how the system uses solar energy to heat water by capturing the minute elements of its design and operation. Software called Transient Systems Simulation (TRNSYS) was used to carefully create the model. Among the most often used simulation system programs is TRNSYS. It was first created by Duffy Beckman in 1935. This is a broad and flexible simulation system that deals mainly with systems showing transient behaviour such as solar energy applications, thermal analysis of buildings, electrical systems, HVAC and so on<sup>27</sup>.

In this fragment, a complicated model involving numerous independent components is manipulated to model the FC-SWHs. The model's three core components are the Type 1b component, which mimics the Flat Plate Collector's (FPC) thermal accomplishment; the Type 110 component, which portrays a inconstant speed water pump; and the Type 60d component, which demonstrates a stratified fluid storage tank with one inlet and one the outlet and elective internal heaters and thermal exchangers. The Type 2b differential temperature controller, which manipulates the system in reply to temperature differences, and the Type 14 forcing functions, which comprise the hot water demand profile (Type 14b), the desired hot water temperature (Type 14e), and the immersion heater control signals (Type 14 h) are supplementary components of the model. Furthermore, the

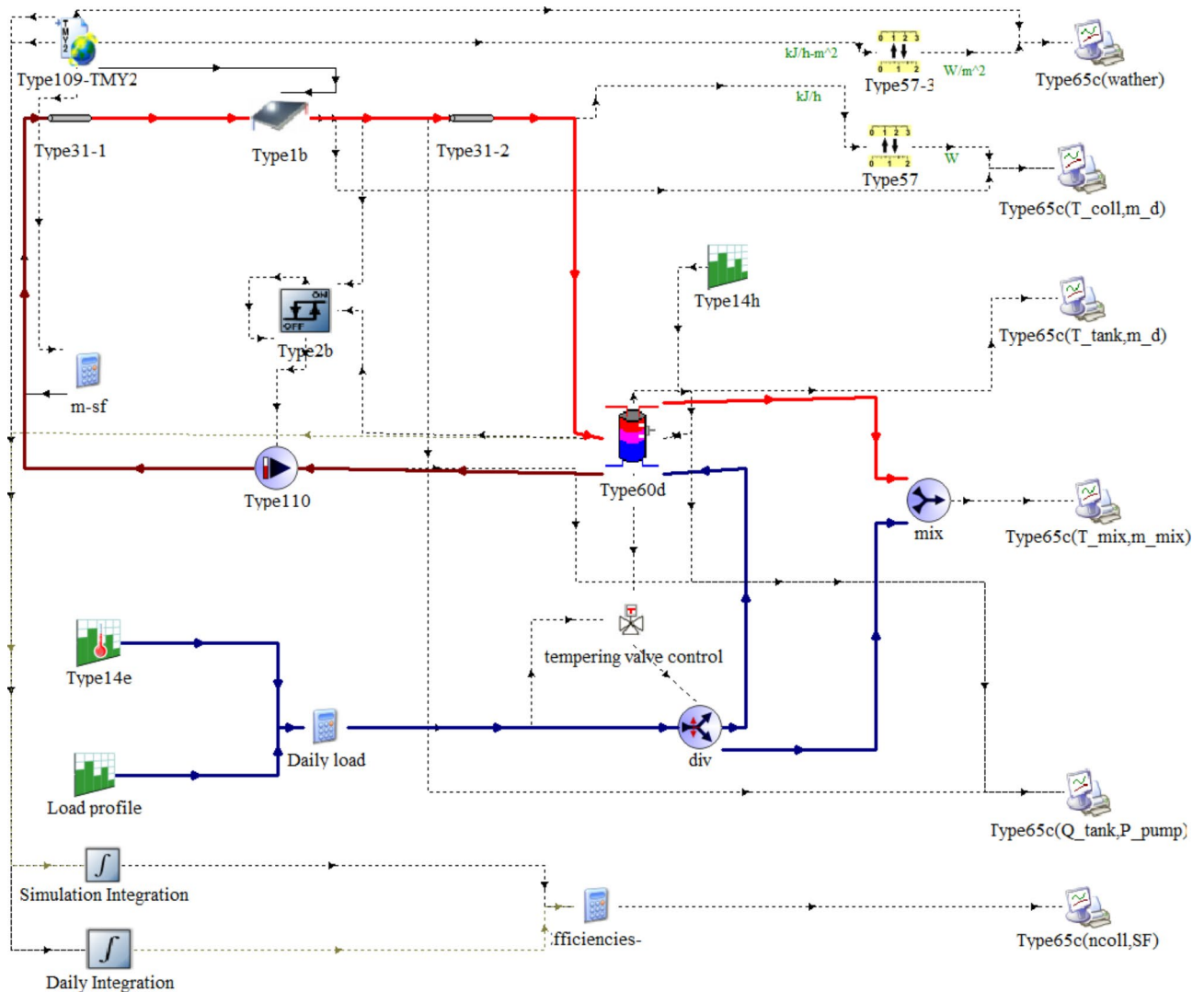


Fig. 3. TRNSYS diagrammatic representation of FC-SWHs.

Type 109-TMY2 weather simulation module, a Type 57 conversion unit, and Type 31 pipelines and ducts for fluid transfer are contained in the simulation model.

To control the flow contained by the system, Type 11f flow diverter, Type 11 h flow mixers and Type 11b temperature-controlled flow diverter is engaged. The Type 24 integrator is used to accumulate system variables over time, while the Type 65c online plotter is repeatedly used to display the results in a comprehensible format. Two Type 24 integrators and Type 65c online plotter with printers are employed to produce output files that encapsulate both daily and cumulative simulation results. The model is further refined by introducing equations for the solar fluid mass flow rate, the daily water load, and the system's efficiency into TRNSYS. The "efficiencies" equation block leverages these integrated values to calculate both daily and overall simulation efficiencies of the collector ( $\eta_{coll}$  and  $\eta_{coll-d}$ ), in addition to daily and total solar energy factors ( $SF$  and  $SF_d$ ). To conclude, a printer/integrator is utilized for the computation of the system's energy balance on a monthly scale. To streamline the process of selecting components for the system, it is essential to construct a diagram that maps out the flow of information. Figure 4 illustrates this diagram, detailing how the components are interconnected and how the data acquisition system is integrated within the setup. The design parameters for the TRNSYS model are detailed across three tables: Table 1 outlines the specifications for the stratified fluid storage tank, Table 2 provides the characteristics of the flat plate collector, and Table 3 lists the variables for the variable speed water pump<sup>28</sup>.

## Results and discussions

This part describes the simulation results for a forced circulation solar water heating system (FC-SWHs). The analysis seeks to predict the FC-SWHs' year-long working under the climatic environments of Ain Témouchent, Algeria. It analyses the influence on separate accomplishment metrics of FC-SWHs thru the year.

### Model validation

The ratification of the FC-SWHs model contained by the TRNSYS simulation framework is a vital stage to guarantee the precision and trustworthiness of the system's functioning estimation. Figure 5 specifies a particularized comparative analysis between the present TRNSYS numerical outcomes and the empirical data from the study operated by Ayompe et al.<sup>28</sup> observing the Collector Outlet Temperature. The temperature projected by the present model indicates a strong correlation with the temperature outcomes from the investigation by Ayompe et al.<sup>28</sup>, representing a superior level of agreement.

### Meteorological data

The estimates consumed a Typical Meteorological Year (TMY) dataset for Ain Témouchent to model the system's annual implementation. Figure 5 demonstrates the monthly variations in meteorological data, with part (a) indicating beam irradiance and part (b) describing wind speed differences. The Mean Beam Irradiance was logged at almost 256.40 W/m<sup>2</sup>. Moreover, the average ambient temperature was noted to be 18.21 °C, and the average wind speed was measured at 2.27 m/s.

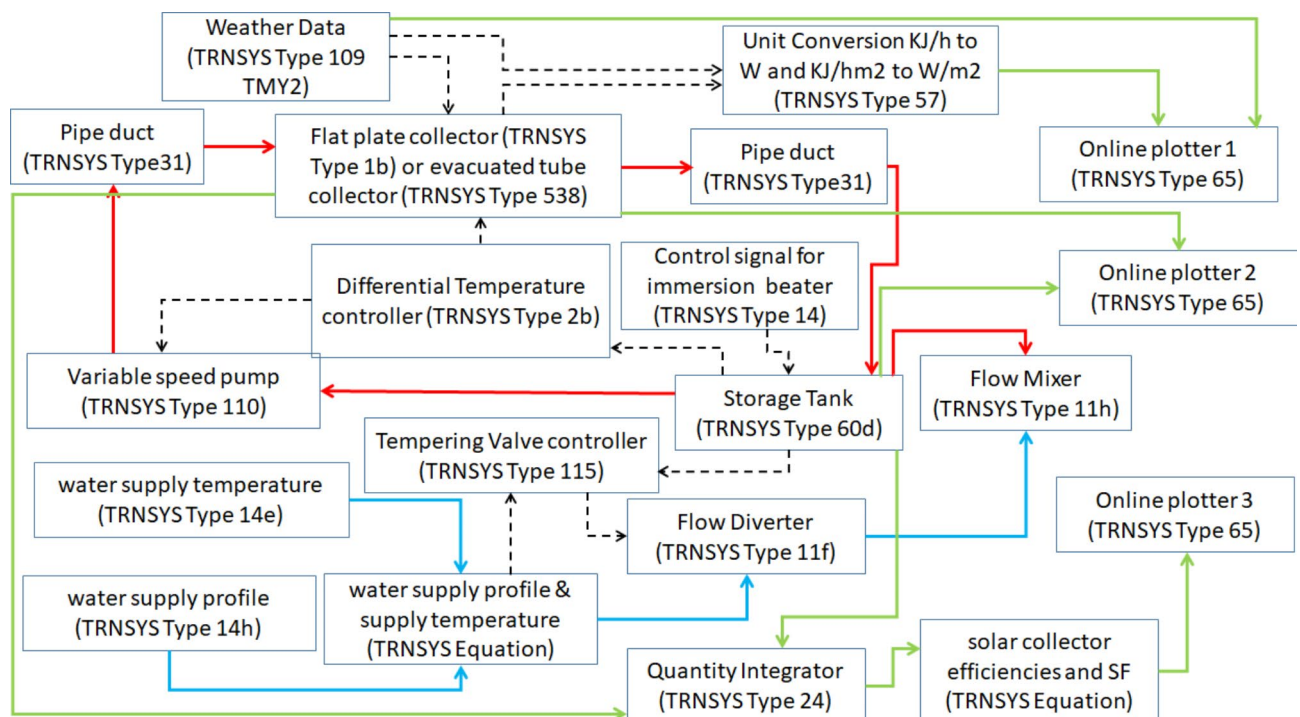


Fig. 4. TRNSYS information flow diagram.



Parameter	Value
Tank volume (m <sup>3</sup> )	0.2
Tank height (m)	1.68
Height of flow inlet (m)	0.1
Height of flow outlet (m)	1.6
Fluid specific heat (kJkg <sup>-1</sup> K <sup>-1</sup> )	4.190
Fluid density (kgm <sup>-3</sup> )	1000
Tank loss coefficient (W m <sup>-2</sup> K <sup>-1</sup> )	0.3
Fluid thermal conductivity (kJhr <sup>-1</sup> m <sup>-1</sup> K <sup>-1</sup> )	1.40
Boiling temperature (C)	100
Height of 1 <sup>st</sup> auxiliary heater (m)	1
Height of 1 <sup>st</sup> thermostat (m)	1.5
Set point temperature for element 1(C)	60
Dead band for heating element 1(C)	5
Maximum heating rate of element 1 (KW)	2.75
Fraction of glycol	0.4
Heat exchanger inside diameter (m)	0.016
Heat exchanger outside diameter (m)	0.02
Heat exchanger fin diameter (m)	0.02
Total surface area of heat exchanger (m <sup>2</sup> )	2
Heat exchanger length (m)	32
Heat exchanger wall thermal conductivity (Wm <sup>-1</sup> K <sup>-1</sup> )	0.5
Heat exchanger material conductivity (WmK <sup>-1</sup> )	0.5
Height of heat exchanger inlet (m)	1
Height of heat exchanger outlet (m)	0

**Table 1.** Stratified fluid storage tank (Type 60d) parameters.<sup>28</sup>

Parameter	Value
Number in series	1
Collector absorber area (m <sup>2</sup> )	2
Fluid specific heat (kJkg <sup>-1</sup> K <sup>-1</sup> )	3.708
Tested flow rate (kghr <sup>-1</sup> m <sup>-2</sup> )	80
Intercept efficiency	0.776
First order efficiency coefficient (Wm <sup>-2</sup> K <sup>-1</sup> )	3.95
Second order efficiency coefficient (Wm <sup>-2</sup> K <sup>-2</sup> )	0.0165
Maximum flow rate (kghr <sup>-1</sup> )	100
Incidence angle (Degrees)	45

**Table 2.** Flat plate collector (Type 1b) parameters.<sup>28</sup>

Parameter	Value
Rated flow rate (kg hr <sup>-1</sup> )	100
Collector absorber area (m <sup>2</sup> )	2
Rated power (kW)	0.063

**Table 3.** Variable speed water pump (type 3b) parameters.<sup>28</sup>

Figure 6(A) depicts the annual fluctuation of beam irradiance. The peak mean solar beam irradiation occurs from June to August, with values ranging from 314.68 W/m<sup>2</sup> to 371.12 W/m<sup>2</sup>. Conversely, December experiences the lowest solar radiation at this location. From January to May, the irradiance varies from 201.73 W/m<sup>2</sup> to 280.79 W/m<sup>2</sup>. Additionally, Fig. 6(B) presents the wind speed variation over the year. The highest wind speed variation recorded is 14.8 m/s in September. In January and October, the maximum wind speed approximates to 13.6 m/s. During the remaining months, the peak wind speeds fluctuate between 14.1 m/s and 14.7 m/s. This data indicates a relatively stable pattern of high wind speeds throughout the year, with slight variations, which could be significant for the design and operation of wind-sensitive structures and systems. The wind

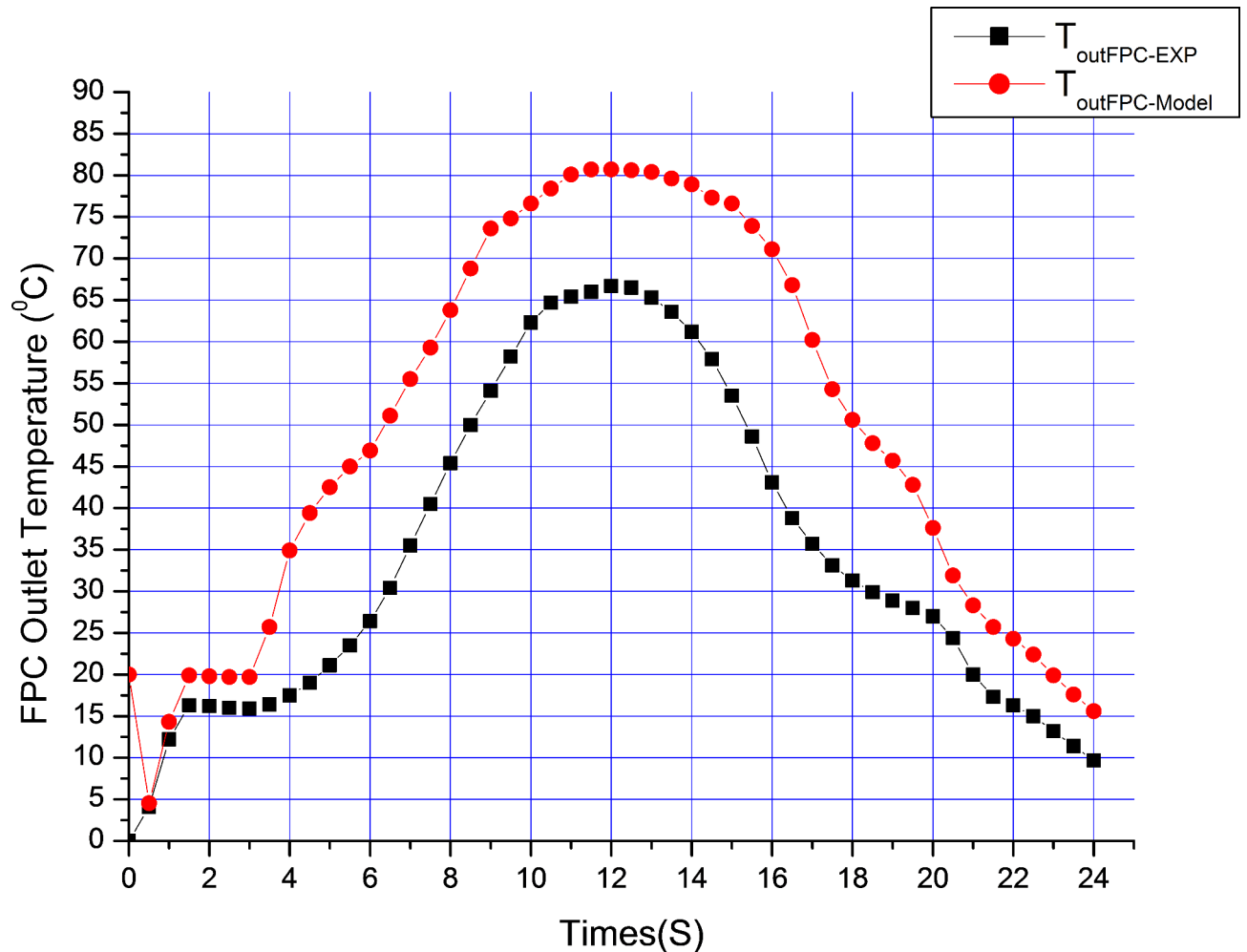


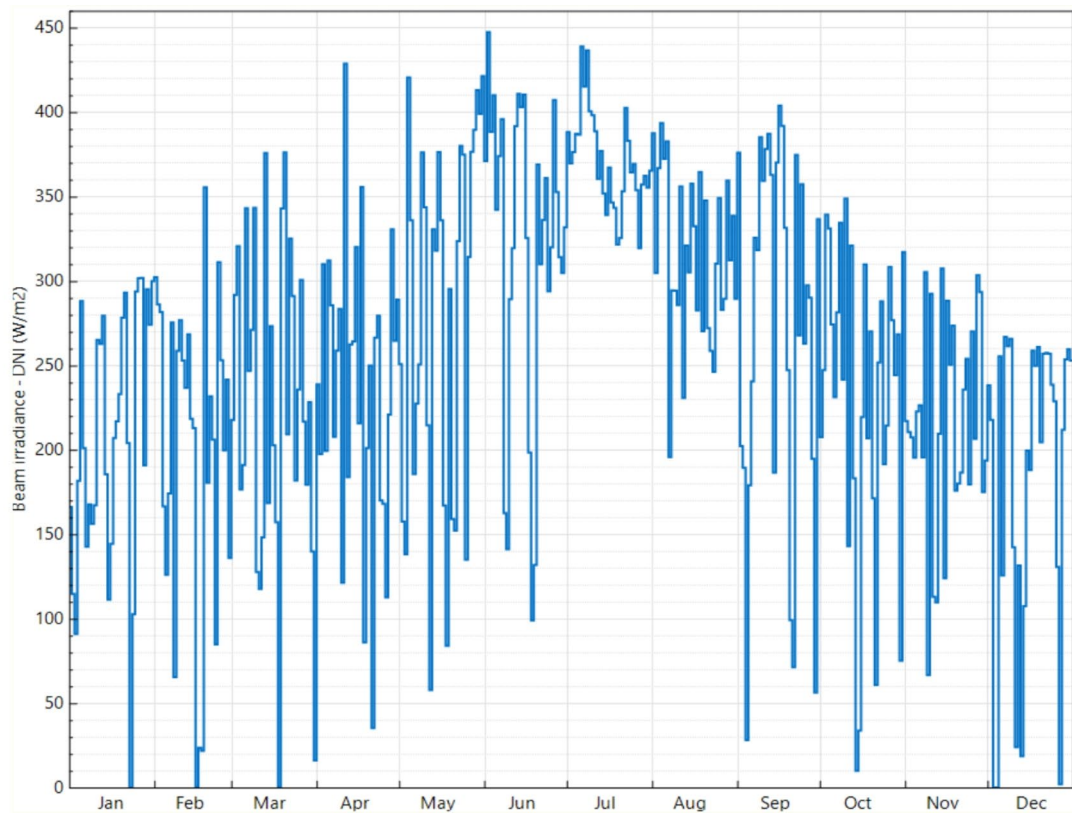
**Fig. 5.** Comparative Analysis of Current TRNSYS Simulations and Experimental Data by Ayompe et al.<sup>28</sup>, for Validating Collector Outlet Temperature.

speeds you've mentioned are within the typical design limits for FC-SWHs. These systems are generally robust and can handle a variety of weather conditions, but extreme wind speeds could potentially affect the system's performance, especially if they exceed the structural design limits or impact the heat collector efficiency.

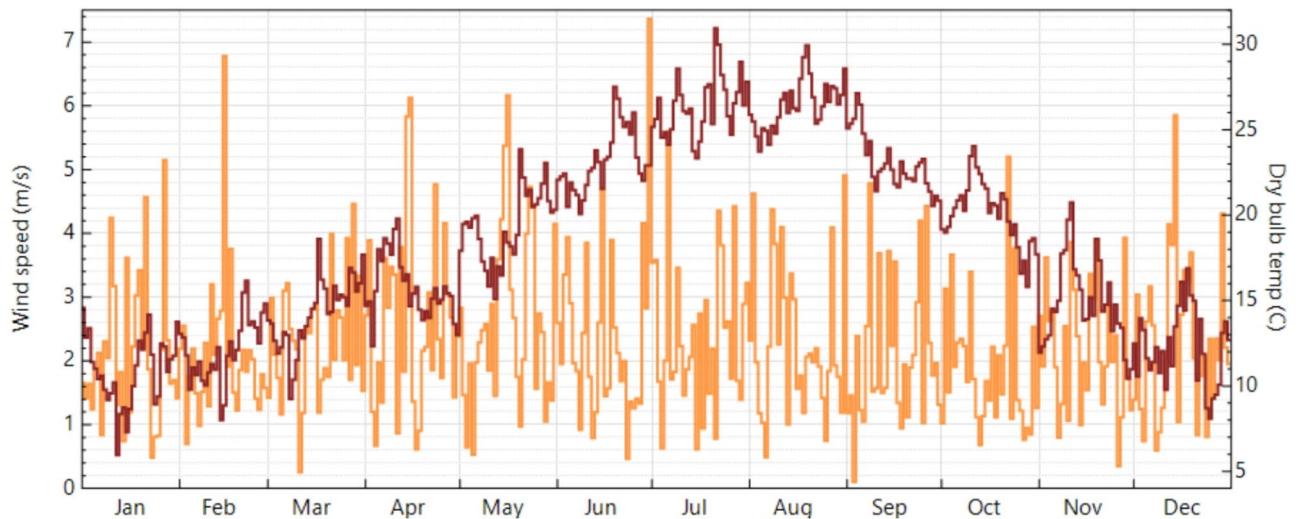
Figure 7 offers a comprehensive view of the monthly average weather statistics, with the left side detailing airstream speed plus ambient air heat, and the right side showing the total solar radiation received by a tilted surface. The wind speed maintains a steady monthly average of 2.5 m/s. The ambient air temperature peaks at an average of 26.25 °C during July and August, while the lowest average temperature hovers around 11 °C in January and December. The total solar radiation received on tilted surfaces varies throughout the year, typically ranging from 210 to 260 W/m<sup>2</sup>. The greatest solar radiation is witnessed at 260 W/m<sup>2</sup> in the months of August and September. This increment can be ascribed to the Earth's angle and its orbit, which consequence in more direct sunlight during these months. Contrariwise, solar radiation occurrences a steady rise between 220 and 250 W/m<sup>2</sup> from January to March, representing the change from winter to spring, where the days happen to be prolonged and the sun's location in the sky elevations. Subsequent this period, there is a minor decline to 230 W/m<sup>2</sup> in May and June, which could be affected by numerous atmospheric circumstances, involving cloud cover and the angle of solar occurrence. As the year continues, solar radiation once more scales to its yearly climax in August and September, reaching the previously elevated of 260 W/m<sup>2</sup>. After this attainment, the radiation levels initiate a falloff, ultimately attaining the lowest of 210 W/m<sup>2</sup> in December, corresponding with the arrival of winter and the shortest days of the year. This cyclical configuration of solar radiation is essential for solar energy systems, as it influences the total of energy that can be exploited and used. Comprehending these differences assists in planning and improving solar installations for extreme productivity thru the year.

#### Monthly average collector outlet temperature and aggregate useful energy acquisition

The data accessible in Fig. 8 implies that the monthly average collector outlet temperatures display comparable developments to the solar radiation models. For the location under consideration, the extreme monthly average outlet temperature for the solar collector is documented at 38 °C in September. This climax is probable due to the extraordinary solar irradiance levels throughout the year, which promote to intensified thermal energy



(A)



(B)

**Fig. 6.** Meteorological Data Analysis - (A) Beam Irradiance and (B) Wind Speed Variations.

accumulation by the solar collector. On the other end of the spectrum, the lowest monthly average collector outlet temperatures are monitored throughout the winter months, by 25 °C in January and marginally superior at 25.5 °C in December. These minimal temperatures indicate the diminished strength of solar radiation and quicker daylight hours.

Furthermore, Fig. 8 also delivers an evident illustration of the Monthly aggregate functional energy acquisition for a FPC thru the year. This energy acquisition is directly drawn to the outlines of solar radiation and changes in ambient temperature. In intervals of raised solar radiation, such as in September, the FPC collector is more efficient, securing a significant volume of energy which converts to risen outlet temperatures. In difference, thru

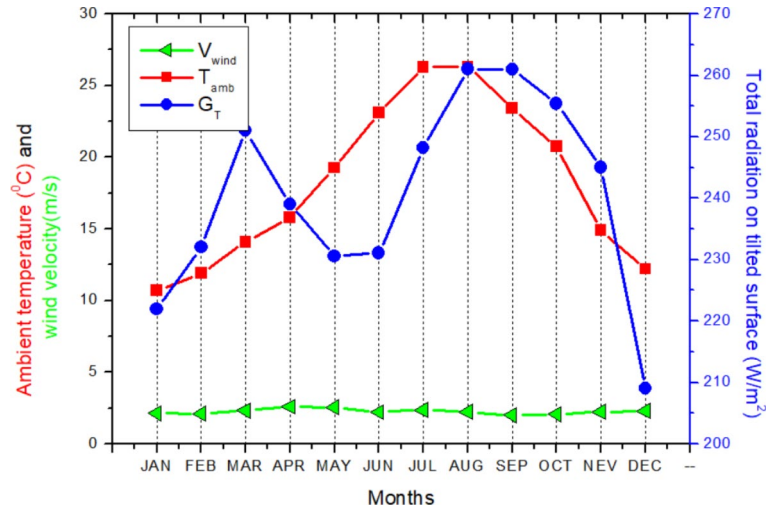


Fig. 7. Monthly average weather data trends for Ain Témouchent - (Left) wind Speed and ambient air temperature; (Right) total solar radiation on tilted surface.

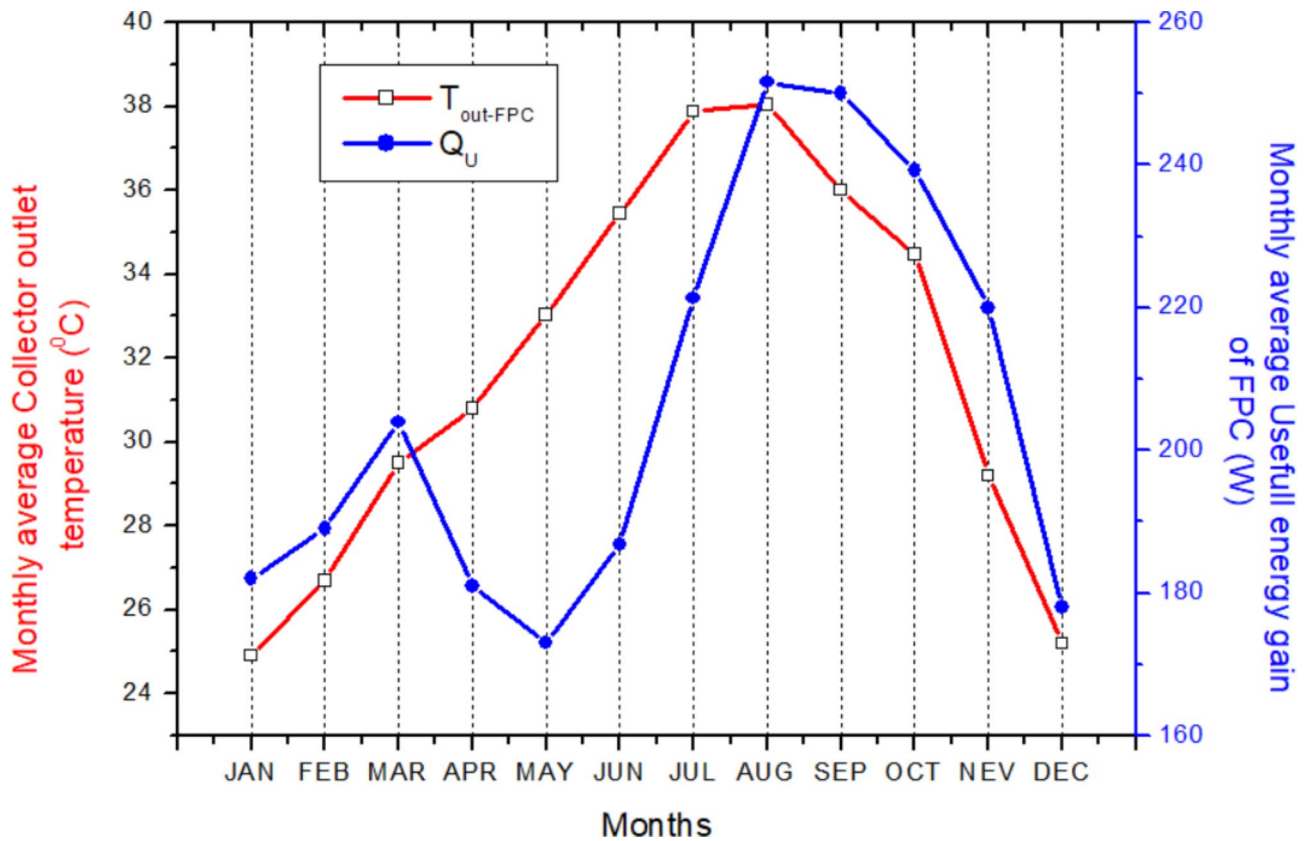


Fig. 8. Monthly average collector outlet temperature (Left) and cumulative useful energy gain (Right).

times when solar radiation is minimum, the energy gained by the FPC collector reduces, which is exhibited in the cooler outlet temperatures. The data indicates that the maximum monthly average cumulative useful energy gain peaks at 250 W in August. The lower bounds of energy gain are noted during the months of January, May, and December, with values of 180 W, 170 W, and 175 W respectively. Moreover, these fluctuations in energy gain mirror the variations in total solar radiation on tilted surfaces as depicted in Fig. 7. The correlation between solar radiation levels and the energy gain of the FPC collector underscores the importance of solar positioning and climate in the efficiency of solar energy systems.

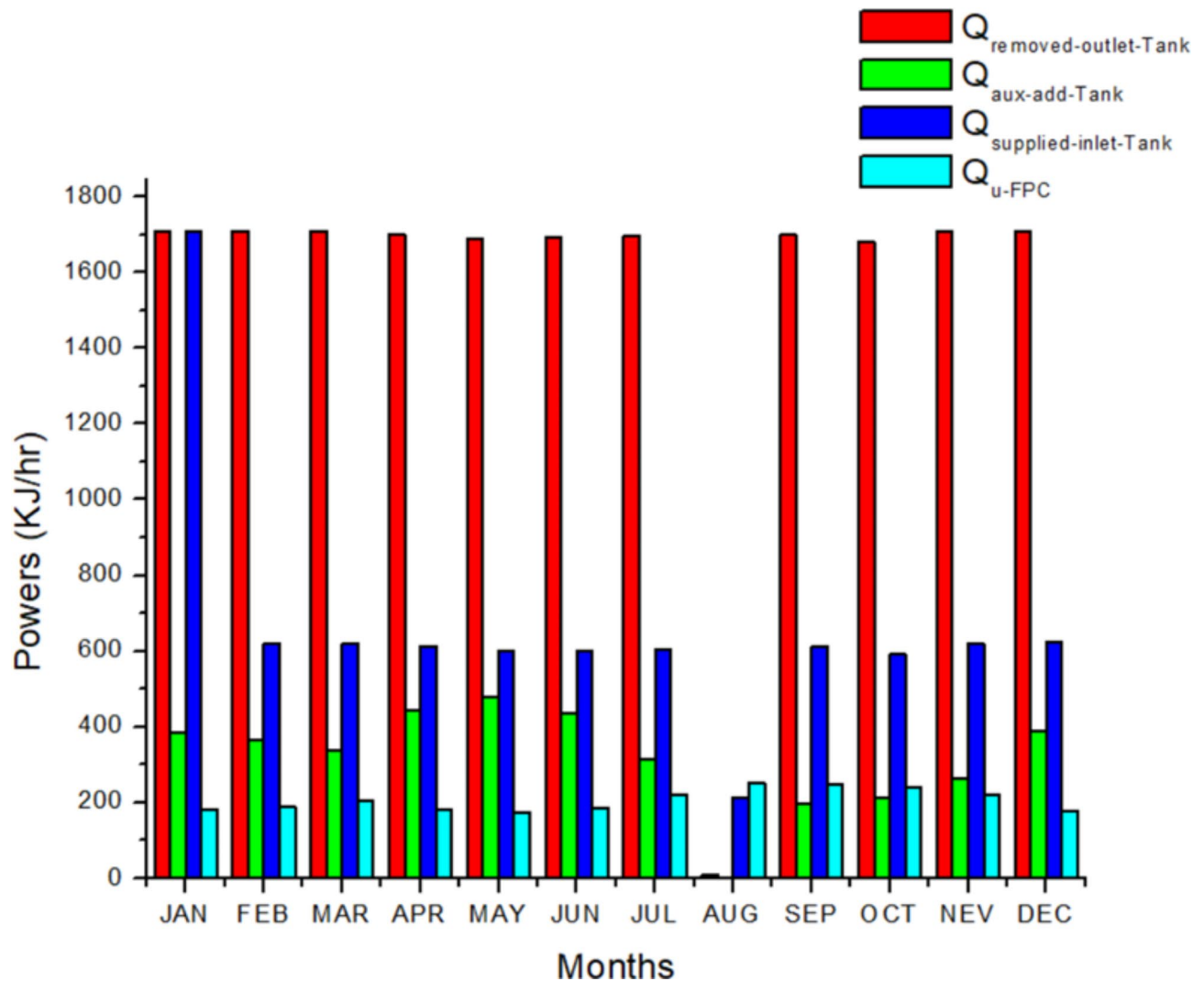
### Average monthly energy supplied through the inlet, extracted through the outlet, auxiliary heating rate, and useful energy gain

Figure 9 delineates the monthly average energy dynamics within a thermal system, detailing the energy transactions via the inlet and outlet, the auxiliary heating contributions, and the FPC's role. Here's a rewritten explanation:

- **Energy Supplied by Inlet ( $Q_{\text{supplied-input-Tank}}$ ):** This represents the rate at which the system's storage tank receives energy, facilitated by the inflow of fluid through the inlet.
- **Energy Removed by Outlet ( $Q_{\text{removed-outlet-Tank}}$ ):** Conversely, this is the rate at which energy is drawn out from the storage tank, corresponding to the outflow of fluid through the outlet.
- **Auxiliary Heating Rate ( $Q_{\text{aux}}$ ):** This metric indicates the average power increment supplied to the tank by the auxiliary heaters.
- **Useful energy gain ( $Q_{\text{u-FPC}}$ ):** refers to the energy harnessed by the Flat Plate Collector (FPC) in a solar thermal system. This energy gain is a measure of the efficiency with which the FPC converts solar radiation into usable heat.

The graphical representation in Fig. 9 provides insights into the thermal performance and energy management within the system. From this figure, it can be found that:

- 1) The auxiliary heating system's energy consumption exhibits a seasonal variation, with the highest consumption rate of 500 kJ/hr occurring in May. This elevated usage suggests that during May, the solar radiation alone may not be sufficient to achieve the desired water temperature of 60 °C, necessitating increased auxiliary heating. In contrast, the lowest consumption rate of 200 kJ/hr is noted in September, which aligns with the period of higher solar radiation. The abundance of solar energy during this time reduces the need



**Fig. 9.** Monthly average of energy supplied through the inlet, extracted through the outlet, auxiliary heating rate, and energy input from the heat exchanger.

- for auxiliary heating, as the solar collectors are likely able to heat the water to the target temperature more efficiently. This pattern indicates that the auxiliary heater's operation is inversely related to the availability of solar radiation; as solar radiation increases, the reliance on auxiliary heating decreases.
- 2) The beneficial dynamism gain ( $Q_{u-FPC}$ ) by the solar collector liquid, as depicted in Fig. 8, demonstrates a correlation with solar radiation, leading to a reduction in the need for auxiliary heating ( $Q_{aux}$ ). It is noteworthy that  $Q_{u-FPC}$  reaches its maximum at 250 W during the month of August, a period when the auxiliary heating consumption ( $Q_{aux}$ ) is negligible. Furthermore, an increase in  $Q_{u-FPC}$  enhances the energy transfer from the Heat Transfer Fluid (HTF) to water ( $Q_{hx}$ ) through the heat exchanger, although this particular process is not illustrated in the figure. This augmentation signifies a more efficient utilization of solar energy, optimizing the system's performance during peak radiation periods.
  - 3) The energy supplied by water at the inlet of the storage tank varies each month, reaching its peak at 500 W in May. This indicates the highest level of energy being introduced into the system via the inlet water during this time. Conversely, the energy input is at its minimum in August, suggesting a lower demand for external energy input due to higher ambient temperatures or increased efficiency of the solar collector during the summer months. This seasonal variation is an important factor in the design and operation of solar thermal systems, as it affects the system's overall energy balance and performance.
  - 4) The energy removed by the outlet of the tank with hot water consistently remains at a high level, due to the steady demand for hot water. This is quantified as being constant at 1700 W for each month. Such consistency in energy removal indicates a stable and continuous need for hot water, which the system is able to fulfill without significant fluctuations throughout the year.

### Average monthly storage tank temperatures

Figure 10 illustrates the monthly average temperatures associated with the storage tank, providing a comprehensive overview of the thermal dynamics within the system. It includes: Outlet temperature of the water exiting the tank, inlet water temperature (bottom), middle tank temperature over the month, HTF temperature at the outlet of HX from the tank and useful water temperature after the mixer (final temperature of the water post-mixing), which is ready for use. The figure indicates that the average outlet water tank temperature maintains a high level within the system, fluctuating between 55 °C and 57 °C. This temperature range is beneficial for consumption when high-temperature water is required. For instances where a lower temperature is needed, the water at the exit of the mixer is consistently maintained at 47 °C, providing a cooler alternative for various uses.

The average bottom water tank temperature is considered the lower-level temperature within the tank, which fluctuates in response to ambient temperature and solar radiation. Over the course of the year, this temperature varies between 36 °C and 38 °C. Following the transfer of energy from the HTF to the water in the tank, there is a noticeable decrease in the HTF's outlet temperature compared to the outlet temperature of the FPC. Consequently, the monthly average outlet temperature of the HTF ranges from 38 °C to 42 °C. This change reflects the heat exchange process's efficiency, where the HTF relinquishes its heat to the water, thereby cooling down before it cycles back to the solar collector.

Figure 10 also presents the monthly average middle temperature of the storage tank, which exhibits variations between 46 °C and 48 °C. This range indicates the intermediate temperature levels within the tank, likely representing the thermal stratification that occurs as the heat is distributed from the top (where water is typically warmer) towards the bottom (where it is cooler). The consistency of this temperature range throughout the year suggests a stable and effective thermal management within the system.

### Average monthly inlet and outlet flow rate of the system

Figure 11 provides a visual representation of the inlet and outlet flow rates of the storage tank, as well as the outlet flow rate from the mixer. The modeling results show that the inlet and outlet flow rates of the tank are equal, which is consistent with the design of a Type 60 storage tank modeled as being completely filled with water. This equality in flow rates is particularly relevant when the system uses water at a high temperature, initially at 55 °C, with a lower flow rate of 7 Kg/hr.

Moreover, the modeling results reveal that the water mass flow rate exiting the mixer is greater than the outlet tank flow rate. This is because it is mixed with cold water to increase the quantity while the temperature is moderated to a lower level, as detailed in Fig. 10. This procedure permits for the modification of water temperature to fit particular usage conditions, guaranteeing that the system can supply hot water at a requested temperature.

### Monthly collector productivity $\eta_{coll}$ and solar fraction SF modification throughout the year

The FC-SWH system is represented in Fig. 12, illustrating the approximate monthly average solar fraction (SF). The data implies that the minimal average SF, at 54%, appears in July, indicating decreased solar heating effectiveness thru this period. Contrarywise, the maximum average SF is witnessed in September, surpassing 84%, which suggests a substantial raise in solar energy consumption. For the balance months, the SF steadily stay beyond 60%, exhibiting a mostly extreme and stable achievement of the FC-SWH system thru the year.

To boost SF of your FC-SWH system, ought to deliberate numerous optimization approaches. Essentially, altering the recirculation flow can be helpful. By interfering the flow thru minimal solar acquisition phases, it can lower excessive heat loss and so advance the SF. Furthermore, sizing the system to guarantee that the collector region and storage tank capacity are balanced to your hot water requirement to uphold productivity. Besides, utilizing dynamic modelling tools like TRNSYS can specify beneficial perceptions into system functioning under unpredictable conditions and parametric findings, permitting for appropriate optimization of the SF. Additionally, improving thermal insulation of the collector and associated piping is a way to reduce heat loss, especially during colder months. Moreover, the orientation of the solar collector. Adjusting the tilt and direction

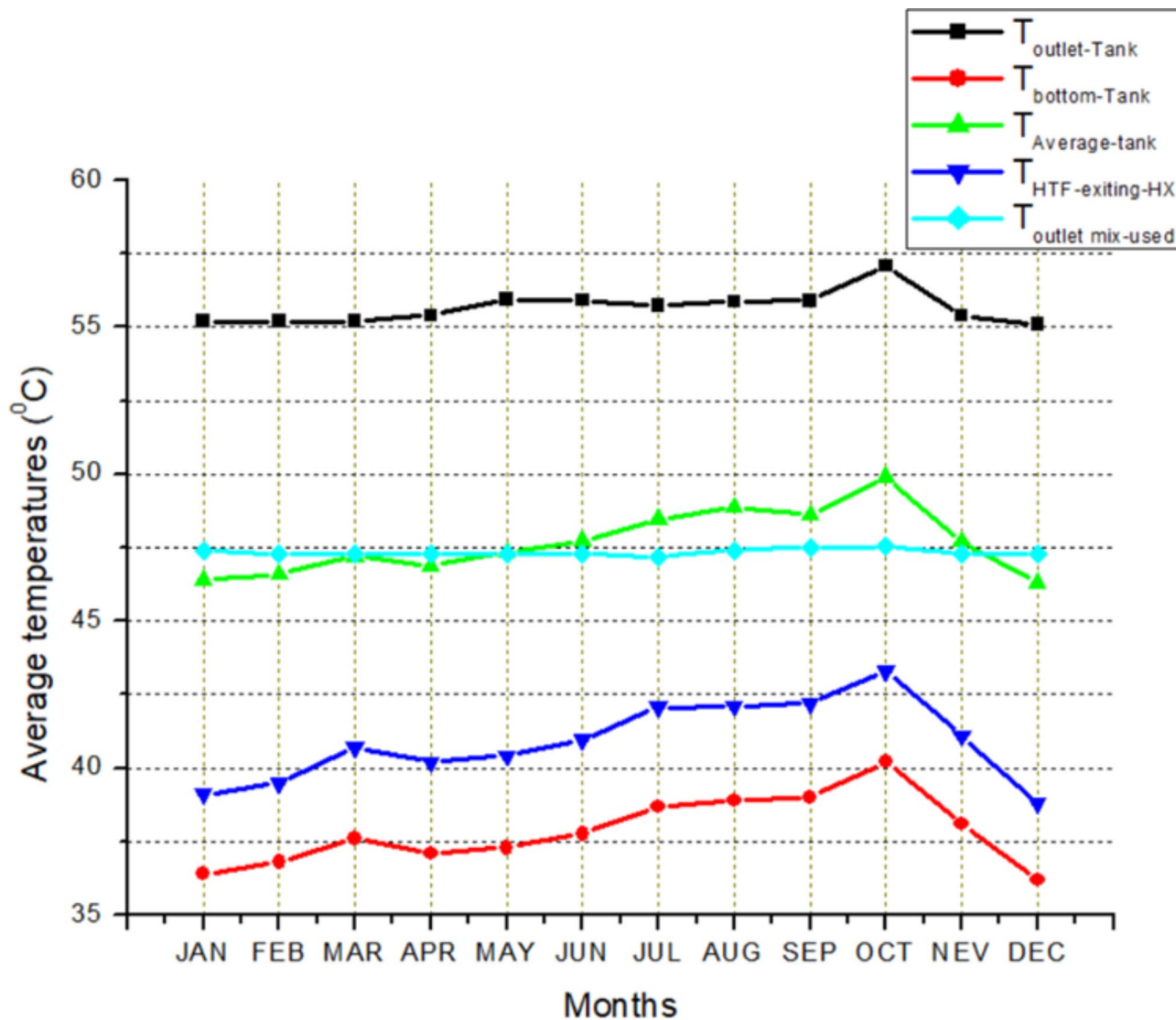


Fig. 10. Monthly average of storage tank temperatures.

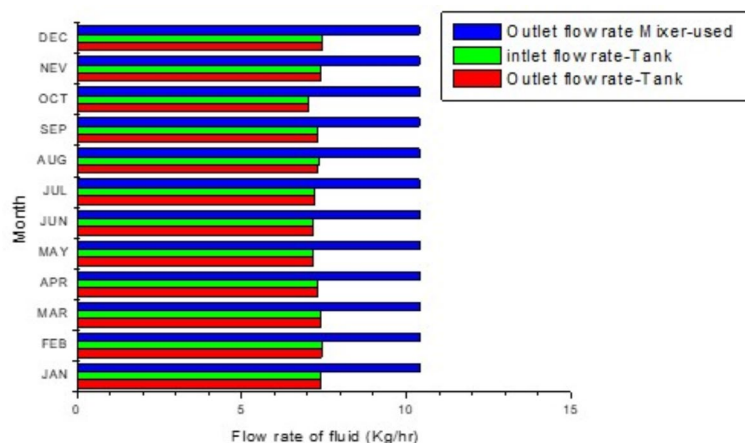
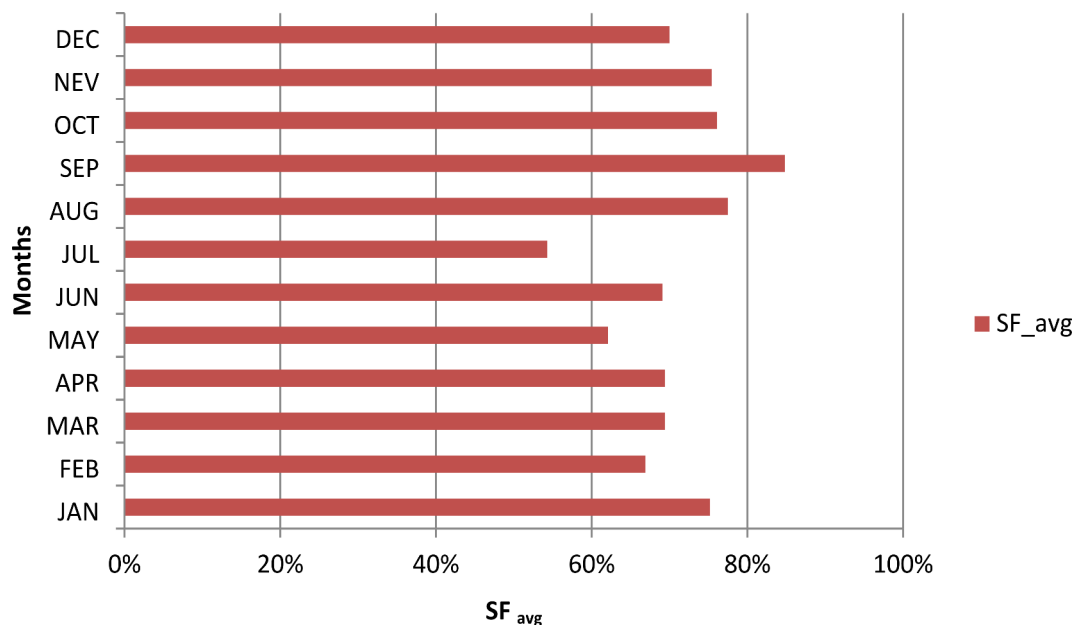


Fig. 11. Monthly average of inlet and outlet flow rate of the system.



**Fig. 12.** Monthly average of solar fraction  $SF$  for the system.

to capture maximum sunlight throughout the year can lead to a higher SF. Lastly, regular maintenance is essential to ensure that all system components are in good working order, preventing efficiency losses over time.

Figure 13 offers an insightful depiction of the simulated performance metrics for FC-SWH system, highlighting its efficiency across different seasonal conditions ( $\eta_{coll}$  and  $SF$ ). (A) January section of the figure presents the system's functionality during the winter months, a period typically associated with lower solar energy availability and heating demands. Moving into (B) April, the figure transitions to illustrate the system's response to spring's milder temperatures and longer daylight hours, which generally improve solar collection. The (C) July portion captures the peak of summer, where the system is likely to experience the highest solar input and efficiency. Lastly, (D) October reflects the beginning of autumn, showcasing the system's adaptability to the decreasing solar radiation as the year progresses.

This figure shows that the total thermal efficiency diminishes and after that stabilizes at a constant value. Additionally, for total SF, it diminishes with fluctuations and abates to constant values. In January (Fig. 13. A), the thermal efficiency of the system ranges between 49% and 73%, indicating a significant variation likely due to environmental or operational factors. As the year progresses, this efficiency shifts to a range of 43–62% in April (Fig. 13. B), suggesting a possible decrease in performance or change in conditions. By July, the efficiency slightly improves, oscillating between 48% and 66% (Fig. 13. C). However, in October, there is an unusual fluctuation, with efficiency starting at a low of 53%, then rising sharply to 53%, and finally reaching up to 69% (Fig. 13. D).

Regarding the total SF, it remains fairly consistent at around 78% in January, which could reflect stable system conditions or effective performance (see Fig. 13. A). In April, SF varies from 65 to 79%, and in July, it further increases, ranging from 62 to 81% (see Fig. 13. B and C). This upward trend continues into October, where SF significantly rises, spanning from 70% to as high as 92% (Fig. 13. D). These percentages suggest that the system's SF is generally robust, with October showing the highest efficiency gains, which could be attributed to specific operational improvements or seasonal impacts on the system's performance.

## Conclusion

The investigation into a forced circulation solar water heating system (FC-SWHs) suitable for the Algerian climate has culminated in the development of a dynamic and robust numerical simulation model. This model, which has been corroborated with literature concerning the collector outlet temperature, shows considerable potential in augmenting the efficiency of hot water supply systems for residential use in Algeria. Anticipated to achieve the hot water obligations of single-family residences with a everyday utilization of 246 L, the model is an evidence to the flexibility of solar heating resolutions to local ecological circumstances. This model, validated against literature, shows potential to enhance hot water supply efficiency for residential use. It provides insights into seasonal performance variations and energy utilization, demonstrating the system's capability to meet daily hot water demands. The research advances solar water heating technology and offers a practical framework for similar climates, contributing to sustainable energy solutions.

The TRNSYS simulation models, crafted to reflect the climatic nuances of Ain Temouchent, Algeria, have yielded pivotal insights:

- The monthly average collector outlet temperatures associate intently with solar radiation developments, summing at 38 °C in September, whereas the winter months score lowest amount of 25 °C in January and 25.5 °C in December.



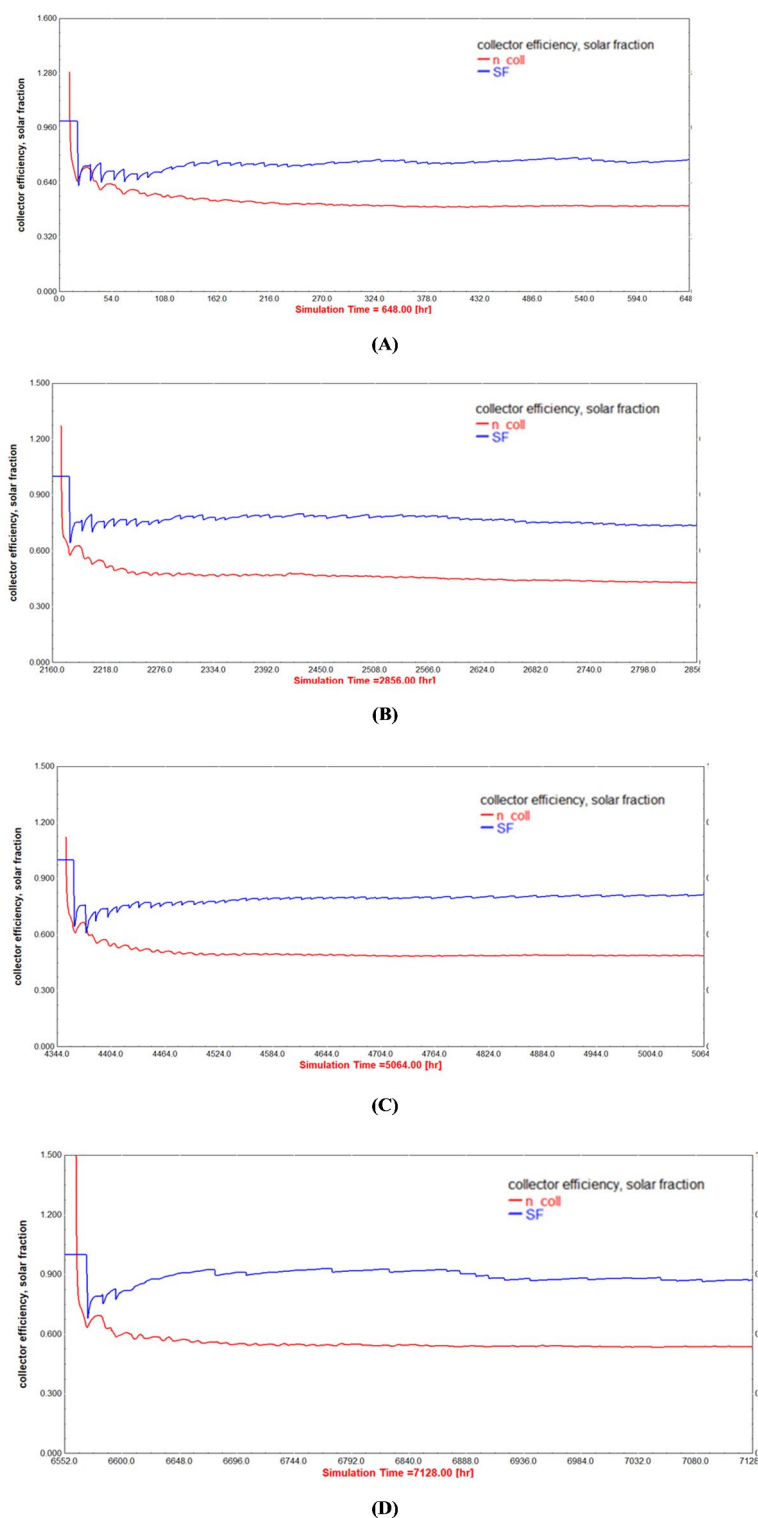


**Fig. 13.** Overall simulation FPC efficiencies  $\eta_{coll}$  and total solar fraction  $SF$  of the system (A). January, (B). April, (C). July, and (D). October.

- The utmost monthly average aggregate practical energy collects attains 250 W in August, with the minimal spectrum of energy collects witnessed in January, May, and December, at 180 W, 170 W, and 175 W respectively.
- Seasonal variations in the supplementary heating system's energy utilization are obvious, with the most important requirement of 500 kJ/hr at May to uphold a water temperature of 60 °C.
- The energy stored at the storage tank's inlet changes monthly, reaching an extreme of 500 W in May.

- The energy removed at the hot water outlet of the tank stays constantly extreme at 1700 W monthly, displaying the continuous hot water requirement.
- The system's average outlet water tank temperature stays constantly extreme, swinging between 55 °C and 57 °C. This scale is beneficial for situations needing hot water. Contrarywise, when a minimal temperature suits, the mixer's withdraw water is consistently maintained at 47 °C, presenting a useful solution for miscellaneous requirements.
- The average bottommost water tank temperature, indicating the tank's minimal thermal stratum, changes starting 36 °C to 38 °C. In the meantime, the monthly average outlet temperature of the Heat Transfer Fluid (HTF) covers between 38 °C and 42 °C, then the storage tank's center temperature sway among 46 °C to 48 °C.
- A notable viewpoint of the system's control is the stability concerning the inlet and outlet flow ratios of the tank, specifically important when the system circulates water at an initial extreme temperature of 55 °C with a flow rate of 7 kg/hr. In difference, the water mass flow proportion leaving the mixer better the outlet tank flow ratio, displaying at 10.5 kg/hr.
- The solar fraction (SF) and thermal productivity metrics demonstrate the system's efficiency. The minimal average SF, at 54%, is documented in July, but September observes the utmost average SF, beyond 84%—evidence to the significant improve in solar energy gain. For the remainder of the year, the SF constantly stays higher than 60%.
- Thermal productivity stages a seasonal range, with January figures vary between 49% and 73%, April's productivity reaches over 43–62%, July's among 48–66%, and October's commencing 53–69%. These data confirm the system's trustworthy working and its rightness for the Algerian weather, guaranteeing competent solar heating throughout the year.

## Data availability

All data generated or analysed during this study are included in this published article.

Received: 3 September 2024; Accepted: 19 November 2024

Published online: 22 November 2024

## References

1. Pahlavan, S., Jahangiri, M., Alidadi Shamsabadi, A. & Khechekhouche, A. Feasibility study of solar water heaters in Algeria, a review. *J. Solar Energy Res.* **3**(2), 135–146 (2018).
2. Haffaf, A. & Lakdja, F. Feasibility and performance analysis of using Solar Water Heating System in Algeria. *UPB Sci. Bull. Ser. C Electr. Eng. Comput. Sci.* **84**, 271–286 (2022).
3. Eze, F. et al. A review on solar water heating technology: impacts of parameters and techno-economic studies. *Bull. Natl. Res. Centre.* **48**(1), 1–22 (2024).
4. Ben Taher, M. A., Kouksou, T., Zeraoui, Y., Ahachad, M. & Mahdaoui, M. Energetic, economic and environmental analysis of domestic solar water heating systems under the African continent. *Int. J. Environ. Sci. Technol.*, pp.1–16. (2021).
5. Mounir, A., Rima, Z. & Aziz, N. Technical-Economic Analysis of Solar Water Heating Systems at Batna in Algeria. In *Sustainability in Energy and Buildings: Proceedings of the 4th International Conference in Sustainability in Energy and Buildings (SEB' 12)*(pp. 787–796). Springer Berlin Heidelberg. (2013).
6. Sami-Mecheri, S., Semmar, D. & Hamid, A. Determination of the energetic needs of low energy housing and integration of a solar water heating installation located in Algeria. *Energy Procedia.* **74**, 854–863 (2015).
7. Ko, M. J. A novel design method for optimizing an indirect forced circulation solar water heating system based on life cycle cost using a genetic algorithm. *Energies* **8**(10), 11592–11617 (2015).
8. Sakellariou, E. I., Axaopoulos, P. J., Bot, B. V. & Kavadias, K. A. First Law Comparison of a Forced-Circulation Solar Water Heating System with an Identical Thermosyphon. *Energies*, **16**(1), p.431. (2022).
9. Allouhi, A., Amine, M. B., Buker, M. S., Kouksou, T. & Jamil, A. Forced-circulation solar water heating system using heat pipe-flat plate collectors: energy and exergy analysis. *Energy* **180**, 429–443 (2019).
10. Wangchuk, K., Dorji, C., Lhendup, T. & THE EFFECT OF PRESET STORAGE TANK TEMPERATURE ON THE STAGNATION OF A FORCED CIRCULATION TYPE SOLAR WATER HEATING SYSTEM. *J. Appl. Eng. Technol. Manage.*, **2**(1), 78–90. (2022).
11. Ibrahim, I. D. et al. *Modelling and Performance Evaluation of a Parabolic Trough Solar Water Heating System in Various Weather Conditions in South Africa* 25pe02318 (Scientific African, 2024).
12. Laasri, I. A., Charai, M., Mghazli, M. O. & Outzourhit, A. Energy performance assessment of a novel enhanced solar thermal system with topology optimized latent heat thermal energy storage unit for domestic water heating. *Renewable Energy*, **224**, p.120189. (2024).
13. Hachchadi, O., Rouse, D. R., Irandoostshahrestani, M. & Mechaqrane, A. Techno-economic assessment and environmental impact of photovoltaic and conventional solar water heating systems in cold climates. *Energy Conversion and Management*, **297**, p.117725. (2023).
14. Suwaed, M. S., Alturki, S. F., Ghareeb, A., Al-Rubaye, A. H. & Awad, O. I. Techno-economic feasibility of various types of solar collectors for solar water heating systems in hot and semi-arid climates: a case study. *Results in Engineering*, **20**, p.101445. (2023).
15. Maraj, A. Experimental validation of a forced-circulation Solar Water Heating System equipped with flat-plate solar collectors—case study. *Eur. J. Eng. Technol. Res.* **5**(5), 565–570 (2020).
16. Qing, L., Ming, L., Chaofeng, X. & Runsheng, T. Modeling and experimental studies on forced circulation solar water heating systems. In *Proceedings of ISES World Congress 2007 (Vol. I–Vol. V) Solar Energy and Human Settlement*(pp. 2108–2111). Springer Berlin Heidelberg. (2009).
17. University of Wisconsin–Madison. (n.d.). TRNSYS: Transient System Simulation Tool. Retrieved May 5, 2024, from: <http://sel.me.wisc.edu/trnsys>
18. Mabrouki, J. et al. Study, simulation and modulation of solar thermal domestic hot water production systems. *Model. Earth Syst. Environ.* **8**(2), 2853–2862 (2022).
19. Al-Madhhachi, H. S., Ajeena, A. M. & Al-Bughaebi, N. A. Dynamic simulation and energy analysis of forced circulation solar thermal system in two various climate cities in Iraq. *AIMS Energy*, **9**(1). (2021).
20. Abdunnabi, M. J. R., Alakder, K. M. A., Alkishriwi, N. A. & Abughres, S. M. Experimental validation of forced circulation of solar water heating systems in TRNSYS. *Energy Procedia.* **57**, 2477–2486 (2014).
21. Yan, Y. et al. Research on solar water heating system based on TRNSYS simulation optimization. *J. Mines Met. Fuels*, **69**(4). (2021).
22. Hobbi, A. & Siddiqui, K. Optimal design of a forced circulation solar water heating system for a residential unit in cold climate using TRNSYS. *Sol. Energy*, **83**(5), 700–714 (2009).

23. Harrabi, I., Hamdi, M., Bessifi, A. & Hazami, M. Dynamic modeling of solar thermal collectors for domestic hot water production using TRNSYS. *Euro-Mediterranean J. Environ. Integr.* **6**, 1–17 (2021).
24. Bernardo, L. R., Davidsson, H. & Karlsson, B. Retrofitting domestic hot water heaters for solar water heating systems in single-family houses in a cold climate: a theoretical analysis. *Energies* **5**(10), 4110–4131 (2012).
25. Jodeiri, A. M. et al. Numerical and experimental investigation of stratified water storage tanks: An enhanced adaptive-grid model. *Applied Thermal Engineering*, 248, p.123113. (2024).
26. Ayompe, L., Duffy, A., McCormack, S., McKeever, M. & Conlon, M. Comparative Field Performance Study of Flat Plate and Heat Pipe Evacuated Tube Collectors (ETCs) for Domestic Water Heating Systems in a Temperate Climate. *Energy*, Vol. 36, Issue 5, pp. 3370–3378. May, doi: (2011). <https://doi.org/10.1016/j.energy.2011.03.034>
27. Shrivastava, R. L., Kumar, V. & Untawale, S. P. Modeling and simulation of solar water heater: a TRNSYS perspective. *Renew. Sustain. Energy Rev.* **67**, 126–143 (2017).
28. Ayompe, L., Duffy, A., McCormack, S. & Conlon, M. Validated TRNSYS model for Forced Circulation Solar Water Heating Systems with flat plate and Heat Pipe evacuated tube collectors. *Appl. Therm. Eng.* **31**, 8–9. <https://doi.org/10.1016/j.applthermaleng.2011.01.046> (June, 2011).

## Acknowledgements

The authors extend their appreciation to the Deanship of Research and Graduate Studies at King Khalid University for funding this work through Large Research Project under grant number RGP2/334/45.

## Author contributions

AR and DN formulated the problem. BK and NAAMN solved the problem. AR, DN, BK, NAAMN, AAE, NA, FAAES and SMH computed and scrutinized the results. All the authors equally contributed in writing and proof reading of the paper. All authors reviewed the manuscript.

## Declarations

## Competing interests

The authors declare no competing interests.

## Additional information

**Correspondence** and requests for materials should be addressed to A.A.-E.

**Reprints and permissions information** is available at [www.nature.com/reprints](http://www.nature.com/reprints).

**Publisher's note** Springer Nature remains neutral with regard to jurisdictional claims in published maps and institutional affiliations.

**Open Access** This article is licensed under a Creative Commons Attribution-NonCommercial-NoDerivatives 4.0 International License, which permits any non-commercial use, sharing, distribution and reproduction in any medium or format, as long as you give appropriate credit to the original author(s) and the source, provide a link to the Creative Commons licence, and indicate if you modified the licensed material. You do not have permission under this licence to share adapted material derived from this article or parts of it. The images or other third party material in this article are included in the article's Creative Commons licence, unless indicated otherwise in a credit line to the material. If material is not included in the article's Creative Commons licence and your intended use is not permitted by statutory regulation or exceeds the permitted use, you will need to obtain permission directly from the copyright holder. To view a copy of this licence, visit <http://creativecommons.org/licenses/by-nc-nd/4.0/>.

© The Author(s) 2024